Polarization switching in an anisotropic cavity coherently pumped $J=1\rightarrow J'=0$ laser

C. Serrat and R. Vilaseca
Departament de Física i Enginyeria Nuclear, Universitat Politècnica de Catalunya, Colom 11, E-08222 Terrassa, Spain

G. J. de Valcárcel and E. Roldán
Departament d'Òptica, Universitat de València, Dr. Moliner 50, E-46100 Burjassot, Spain

(Received 24 February 1997)

We show that, in an optically pumped resonant $J=1\rightarrow J'=0$ laser, a gain anisotropy is induced by a linearly polarized coherent pump beam that can be balanced or countered by x-y cavity-loss anisotropies, leading to switching between the x and y linearly polarized states of the generated laser field as the laser intensity is increased. This switching is not brought about by selection of the mode with the maximum emission intensity. A domain of bistability between the two linearly polarized states is found, whose width depends on the value of the decay rate of the two photon coherence induced among the sublevels of the $J=1$ level manifold. Differently from the incoherently pumped $J=1\rightarrow J'=0$ laser, the decay rate for the magnetic dipole in that manifold has no influence on the polarization of the emission. [S1050-2947(97)06309-9]

PACS number(s): 42.65.Pc, 42.65.Sf, 42.60.Mi, 42.55.Lt

I. INTRODUCTION

In the field of laser dynamics, there is presently a great deal of interest in studying the dynamics of the *vector* field, i.e., in considering variations not only in the power and spatial pattern and frequency of the laser emission, but also in the polarization state of the electric field. Besides their fundamental interest, polarization phenomena such as switching between orthogonally polarized states, bistability, periodic evolution, etc., could have applications in different fields because of the small energy variations their control may require.

Laser polarization dynamics can be observed only in systems with small gain and cavity anisotropies or in systems with anisotropies that depend on the operating conditions or emission state of the laser system. So far, polarization dynamics has been observed or predicted in several classes of laser systems: incoherently pumped gas lasers with different $J\rightarrow J'$ atomic transitions [1–8,10,11], coherently (optically) pumped $J=1\rightarrow J'=0$ gas lasers [12,13], fiber lasers [14–16], and VCSEL [17–20] and edge-emitting [21] semiconductor lasers, among others. Recently, the interplay between the polarization state and spatial dependence of the laser field has also been investigated [22,23]. The origin of the anisotropies leading to polarization dynamics as well as the observed behaviors in these systems can be very different from each other.

In the case of $J=1\rightarrow J'=0$ gas lasers, focusing for simplicity on the case of exact cavity resonance, there is a clear difference between incoherently pumped and coherently pumped laser systems. In the first case the gain is in principle nearly isotropic, so that, if the cavity is also isotropic, small details of the field-matter interaction process will be able to influence and even determine the polarization state of the laser light. This has been shown in [6,7], where in order to be able to explain some experimentally observed features (preference for linear or circular polarization, polarization switching between different polarization states) a rigorous model has been used that goes beyond the third-order Lamb theory and takes into account the relaxation processes affecting separately the three rotation-invariant tensorial quantities describing the atomic state in the $J=1$ sublevel manifold. It has been shown in [6,7] that quantitative differences between the decay rates associated with these tensorial quantities can strongly influence the polarization state of the laser light.

By contrast, in the case of an optically pumped $J=1\rightarrow J'=0$ laser, it has been shown in [13] that a linearly polarized pump field (acting on an adjacent $J''=0\rightarrow J=1$ transition) induces a strong gain anisotropy that favors generation of laser light with linear polarization parallel to that of the pump field. This fact makes the appearance of polarization effects more difficult. That study, however, did not take into account separately all the relaxation processes associated to the tensorial quantities of the $J=1$ manifold, which means that the analysis was not general enough. On the other hand, it is not known whether other factors, in particular cavity-loss anisotropies, could counterbalance in some way the pump-induced gain anisotropy, thus making possible the appearance of polarization effects.

In this work we investigate theoretically the possibilities of polarization effects in a resonant $J=1\rightarrow J'=0$ laser, optically pumped by means of a linearly polarized pump field, by considering the influence of two factors: (i) the three relaxation rates $\gamma_{\parallel}$, γ_J, and γ_c corresponding to the total population, magnetic dipole, and ''electric quadrupole'' (tensorial quantities of the $J=1$ level manifold), respectively, and (ii) the presence of cavity-loss anisotropies for the linearly polarized components of the laser field (which can be easily implemented by introducing appropriate elements within the laser cavity), also known as ''x-y anisotropy.'' Our analysis shows that it is the second factor that turns out to play the most important role in determining the polarization in a laser coherently pumped by means of a linearly polarized field. The first factor has a much smaller influence in this case than for the incoherently pumped laser. Other complementary factors that might generate polarization dynamics, such as external modulation of laser parameters [24],

polarization selective external reflectors [20], or application of a magnetic field [13], will not be considered in this work.

II. LASER MODEL

We assume a three-level-Λ atomic medium in which a pump field acts resonantly on a $J''=0 \rightarrow J=1$ transition and a laser field propagating in the same direction is generated on the adjacent transition $J=1 \rightarrow J'=0$. The optical cavity of the laser system is on resonance with the $J=1 \rightarrow J'=0$ transition.

The three-dimensional state space associated with the $J=1$ level is defined by the basis of ''circular'' states $|J_z=+1\rangle \equiv |+\rangle$, $|J_z=-1\rangle \equiv |-\rangle$, and $|J_z=0\rangle \equiv |0\rangle$, or, equivalently, by the basis of ''linear'' states $|x\rangle$, $|y\rangle$, and $|z\rangle$, defined as

$$|x\rangle = (|1\rangle + |-1\rangle)/\sqrt{2},$$
$$|y\rangle = -i(|1\rangle - |-1\rangle)/\sqrt{2}, \quad (1)$$
$$|z\rangle = |0\rangle.$$

If the quantization axis is chosen in the direction of propagation of the optical fields, only the two-dimensional subspace defined by the circular states $|1\rangle$ and $|-1\rangle$ or, equivalently, by the linear states $|x\rangle$ and $|y\rangle$, can be coupled with the $J''=0$ or $J'=0$ states through the interaction with the optical fields. In previous analyses [12,13], the basis of circular states was adopted and, correspondingly, the optical fields were also expressed on a basis of right-handed and left-handed circularly polarized components. In our analysis, however, we are interested in the most common case of linearly polarized fields and linear cavity loss anisotropies [factor (ii) above], so that the basis of states $|x\rangle$, $|y\rangle$ will be more appropriate and the optical fields will also be expressed on a basis of linearly polarized components in the x and y directions. In this form, the interactions $|J''=0\rangle \rightarrow |x\rangle$, $|J''=0\rangle \rightarrow |y\rangle$, $|x\rangle \rightarrow |J'=0\rangle$, and $|y\rangle \rightarrow |J'=0\rangle$ can be described through Rabi frequencies $2\beta_x$, $2\beta_y$, $2\alpha_x$, and $2\alpha_y$, respectively (where β stands for the pump field and α for the laser field). The cavity anisotropy will be introduced by defining different cavity-loss rates κ_x and κ_y for each component α_x and α_y, respectively, of the laser field.

The factor (i) above will be introduced as in [6] by defining relaxation rates $\gamma_\parallel$, γ_J, and γ_c for the following corresponding physical quantities associated with the $J=1$ level manifold: (a) total population $(\rho_{xx}+\rho_{00}+\rho_{yy}) \equiv (\rho_{++}+\rho_{00}+\rho_{--})$, where $\rho_{kk} \equiv \langle k|\rho|k\rangle$, $k=+,-,0,x,y$, and ρ represents the density matrix operator; (b) magnetic dipole $-2\mathrm{Im}\rho_{xy} \equiv (\rho_{++}-\rho_{--})$; (c) ''electric quadrupole'' $(\rho_{xx}+\rho_{yy}-2\rho_{00}) \equiv (\rho_{++}+\rho_{--}-2\rho_{00})$ and intersublevel coherence $(\rho_{xx}-\rho_{yy}-i\rho_{xy}-i\rho_{yx})/2 \equiv \rho_{+-}$, which are components of tensorial quantitites of order 0, 1, and 2, respectively, that remain invariant under rotations of the reference frame or unitary basis transformations [6,25].

Solving the semiclassical Maxwell-Bloch equations in the density-matrix formalism, assuming the usual slowly varying envelope and rotating-wave approximations, and working in the plane-wave and uniform-field limits, the following set of equations is obtained:

$$\dot{\rho}_{11} = -\gamma_\parallel \rho_{11} - i\alpha_x(\rho_{x1}-\rho_{1x}) - i\alpha_y(\rho_{y1}-\rho_{1y}),$$
$$\dot{\rho}_{22} = \gamma_\parallel(1-\rho_{22}) - i\beta_x(\rho_{x2}-\rho_{2x}) - i\beta_y(\rho_{y2}-\rho_{2y}),$$
$$\dot{\rho}_{xx} = -(1/3)[\rho_{xx}(2\gamma_c+\gamma_\parallel) - (\gamma_c-\gamma_\parallel)(\rho_{00}+\rho_{yy})] + i\alpha_x(\rho_{x1}-\rho_{1x}) + i\beta_x(\rho_{x2}-\rho_{2x}),$$
$$\dot{\rho}_{00} = -(1/3)[\rho_{00}(2\gamma_c+\gamma_\parallel) - (\gamma_c-\gamma_\parallel)(\rho_{xx}+\rho_{yy})],$$
$$\dot{\rho}_{yy} = -(1/3)[\rho_{yy}(2\gamma_c+\gamma_\parallel) - (\gamma_c-\gamma_\parallel)(\rho_{xx}+\rho_{00})] + i\alpha_y(\rho_{y1}-\rho_{1y}) + i\beta_y(\rho_{y2}-\rho_{2y}),$$
$$\dot{\rho}_{1x} = -\gamma_\perp \rho_{1x} - i\alpha_x(\rho_{xx}-\rho_{11}) + i\beta_x\rho_{12} - i\alpha_y\rho_{yx}e^{-i\phi},$$
$$\dot{\rho}_{1y} = -\gamma_\perp \rho_{1y} - i\alpha_y(\rho_{yy}-\rho_{11}) - i(\alpha_x\rho_{xy} - \beta_y\rho_{12})e^{i\phi},$$
$$\dot{\rho}_{2x} = -\gamma_\perp \rho_{2x} - i\beta_x(\rho_{xx}-\rho_{22}) - i\beta_y\rho_{yx} + i\alpha_x\rho_{21}, \quad (2)$$
$$\dot{\rho}_{2y} = -\gamma_\perp \rho_{2y} - i\beta_y(\rho_{yy}-\rho_{22}) - i\beta_x\rho_{xy} + i\alpha_y\rho_{21}e^{-i\phi},$$
$$\dot{\rho}_{21} = -\gamma_\perp \rho_{21} + i\alpha_x\rho_{2x} - i\beta_x\rho_{x1} + i(\alpha_y\rho_{2y} - \beta_y\rho_{y1})e^{i\phi},$$
$$\dot{\rho}_{xy} = -(1/2)[\gamma_c(\rho_{xy}+\rho_{yx}) + \gamma_J(\rho_{xy}-\rho_{yx})] - i\beta_x\rho_{2y} + i(\alpha_y\rho_{x1} - \alpha_x\rho_{1y})e^{-i\phi} + i\beta_y\rho_{x2},$$
$$\dot{\alpha}_x = -\kappa_x\alpha_x - g\,\mathrm{Im}(\rho_{1x}),$$
$$\dot{\alpha}_y = -\kappa_y\alpha_y - g\,\mathrm{Im}(\rho_{1y}),$$
$$\dot{\phi}_{1x} = g\,\mathrm{Re}(\rho_{1x})/\alpha_x,$$
$$\dot{\phi}_{1y} = g\,\mathrm{Re}(\rho_{1y})/\alpha_y,$$

where $\rho_{ij} = \langle i|\rho|j\rangle$ ($i,j=1,2,0,x,y$, where 2 stands for the ground state $J''=0$ and 1 stands for the lower laser transition level $J'=0$), $\phi = (\phi_{1x}-\phi_{1y}) - (\phi_{2x}-\phi_{2y})$, where ϕ_{1i} ($i=x,y$) represents the phase of the complex laser field and ϕ_{2i} represents the phase of the complex pump field, $\gamma_\perp$ is the transverse relaxation rate (for the induced atomic coherences ρ_{1x} and ρ_{1y}), and g is the unsaturated gain parameter. The reference frequency for the laser field has been taken to be equal to the empty cavity resonance frequency.

For simplicity, and in order to obtain analytical solutions, it has been assumed that the population decay rate for levels 2 and 1 is the same as for level $J=1$ ($\gamma_\parallel$), the transverse relaxation rate for coherences ρ_{2x}, ρ_{2y}, and ρ_{21} is the same as for coherences ρ_{1x} and ρ_{1y} ($\gamma_\perp$), and the initial population in the upper levels $J=1$ and $J'=0$ is negligible (i.e., $\rho_{xx}=\rho_{yy}=\rho_{00}=\rho_{11}=0$ and $\rho_{22}=1$ at $t=0$). We will also assume that in resonance $\mathrm{Re}(\rho_{1x})$ and $\mathrm{Re}(\rho_{1y})$ are null (i.e., that the frequency of the generated field coincides with that of the cavity and of the $J=1 \rightarrow J'=0$ transition), a point that has been checked numerically.

Equations (2) are different from the equations obtained in [12] not only in the fact that a different basis of states has been used but also in the fact that factors (i) and (ii) above were ignored there. In particular, with respect to factor (i) in

addition to relaxation rates $\gamma_\parallel$ and $\gamma_\perp$, only a relaxation rate γ_{+-} was considered in [12] for the upper-level coherence ρ_{+-}, so that γ_J as well as the population ρ_{00} were absent in the laser equations. Note that here the upper-level coherence is described by the density matrix element ρ_{xy}, which is related to the upper-level coherence in the basis of circular states, ρ_{+-}, by $\rho_{xy}=-i(\rho_{++}-\rho_{--}-\rho_{+-}+\rho_{-+})/2$.

Equations (2) show a fundamental difference between the cases of the incoherently and coherently pumped $J=1\rightarrow J'=0$ laser system: whereas in the first case [6–9] the phase difference $\phi_{1x}-\phi_{1y}$ between the two orthogonal components of the laser field does not appear in the laser equations and thus there is a degeneracy of solutions with respect to the initial polarization state of the laser field, in the present case this phase difference appears through ϕ in the laser equations (2) and thus the laser state is sensitive to the initial polarization of the laser field. This is because the presence of a pump field vector breaks the rotation invariance of the laser medium and introduces a clear reference for the relative phase between the two laser field components.

Equations (2) also provide insight into the possible influence of the relaxation rate γ_J on the behavior of the coherently pumped laser. In the case of linear polarization of the pump field in either the x or y direction (the case to be considered in this work), the parameter γ_J disappears explicitly from Eqs. (2). This can be easily understood in the basis of ''circular'' states $|+\rangle$ and $|-\rangle$: the linearly polarized pump field excites the atoms to a coherent state $|x\rangle$, which according to Eq. (1) has exactly the same projection, in modulus, on the states $|+\rangle$ and $|-\rangle$. Thus, these two states $|+\rangle$ and $|-\rangle$ become equally populated, and this remains so at any time because the relaxation mechanisms do not alter this equality. As a consequence of this fact no magnetic dipole is created and thus the relaxation rate γ_J does not play any role. This relaxation rate would come into play only if the pumping is linearly polarized in directions other than x or y (assuming, in general, $\kappa_x\neq\kappa_y$) or is elliptically or circularly polarized. Thus in our case of pump field linearly polarized in the x or y direction, the parameter γ_J can be made to disappear from Eqs. (2), which, taking into account all comments above, can be expressed in the simpler real form:

$$\dot{\rho}_{11}=-\gamma_\parallel\rho_{11}-2[\alpha_x\mathrm{Im}(\rho_{1x})+\alpha_y\mathrm{Im}(\rho_{1y})],$$

$$\dot{\rho}_{22}=\gamma_\parallel(1-\rho_{22})-2\beta\mathrm{Im}(\rho_{2x}),$$

$$\dot{\rho}_{xx}=(-1/3)[\gamma_c(2\rho_{xx}-\rho_{yy}-\rho_{00})+\gamma_\parallel(\rho_{xx}+\rho_{yy}+\rho_{00})]+2[\alpha_x\mathrm{Im}(\rho_{1x})+\beta\mathrm{Im}(\rho_{2x})],$$

$$\dot{\rho}_{00}=(1/3)[\gamma_c(\rho_{xx}+\rho_{yy}+\rho_{00})-\gamma_\parallel(\rho_{xx}+\rho_{yy}+\rho_{00})],$$

$$\dot{\rho}_{yy}=(-1/3)[\gamma_c(-\rho_{xx}+2\rho_{yy}-\rho_{00})+\gamma_\parallel(\rho_{xx}+\rho_{yy}+\rho_{00})]+2\alpha_y\mathrm{Im}(\rho_{1y}),$$

$$\begin{aligned}
\mathrm{Im}(\dot{\rho}_{1x})&=-\gamma_\perp\mathrm{Im}(\rho_{1x})-\alpha_x(\rho_{xx}-\rho_{11})-\alpha_y\mathrm{Re}(\rho_{xy})+\beta\mathrm{Re}(\rho_{21}),\\
\mathrm{Im}(\dot{\rho}_{1y})&=-\gamma_\perp\mathrm{Im}(\rho_{1y})-\alpha_y(\rho_{yy}-\rho_{11})-\alpha_x\mathrm{Re}(\rho_{xy}),\\
\mathrm{Im}(\dot{\rho}_{2x})&=-\gamma_\perp\mathrm{Im}(\rho_{2x})-\beta(\rho_{xx}-\rho_{22})+\alpha_x\mathrm{Re}(\rho_{21}),\\
\mathrm{Im}\,(\dot{\rho}_{2y})&=-\gamma_\perp\mathrm{Im}(\rho_{2y})-\beta\mathrm{Re}(\rho_{xy})+\alpha_y\mathrm{Re}(\rho_{21}),\\
\mathrm{Re}(\dot{\rho}_{21})&=-\gamma_\perp\mathrm{Re}(\rho_{21})-\beta\mathrm{Im}(\rho_{1x})-\alpha_x\mathrm{Im}(\rho_{2x})-\alpha_y\mathrm{Im}(\rho_{2y}),\\
\mathrm{Re}(\dot{\rho}_{xy})&=-\gamma_c\mathrm{Re}(\rho_{xy})+\alpha_y\mathrm{Im}(\rho_{1x})+\alpha_x\mathrm{Im}(\rho_{1y})+\beta\mathrm{Im}(\rho_{2y}),\\
\dot{\alpha}_x&=-\kappa_x\alpha_x-g\,\mathrm{Im}(\rho_{1x}),\\
\dot{\alpha}_y&=-\kappa_y\alpha_y-g\,\mathrm{Im}(\rho_{1y}),
\end{aligned}\tag{3}$$

where for definiteness it has been assumed that pumping is linearly polarized in the x direction: $\beta\equiv\beta_x$, $\beta_y=0$. Note that now variables ϕ_{1x}, ϕ_{1y}, $\mathrm{Re}(\rho_{2x})$, $\mathrm{Re}(\rho_{2y})$, $\mathrm{Im}(\rho_{21})$, and $\mathrm{Im}(\rho_{xy})$ are zero and have been eliminated from the laser equations. Disappearance of the phase difference $\phi_{1x}-\phi_{1y}$ from the laser equations in this case does not introduce in practice any uncertainty in the laser polarization state, since, as will be shown below, in the operating conditions considered all the stable solutions found are linearly polarized in directions x or y.

III. STEADY-STATE SOLUTIONS AND STABILITY

A. Zero-intensity solution

Equation (3) yield a zero-intensity steady-state solution given by

$$\begin{aligned}
\rho_{22}&=1-6\beta^2\gamma_c/A,\\
\rho_{xx}&=2\beta^2(\gamma_c+2\gamma_\parallel)/A,\\
\rho_{yy}=\rho_{00}&=2\beta^2(\gamma_c-\gamma_\parallel)/A,\\
\mathrm{Im}(\rho_{2x})&=3\beta\gamma_c\gamma_\parallel/A,\\
\rho_{11}=\rho_{1x}=\rho_{1y}&=\mathrm{Im}(\rho_{2y})=\mathrm{Re}(\rho_{21})=\mathrm{Re}(\rho_{xy})=\alpha_x=\alpha_y=0,
\end{aligned}\tag{4}$$

where

$$A=[4\beta^2(2\gamma_c+\gamma_{||})+3\gamma_c\gamma_{||}\gamma_\perp].$$

A linear stability analysis of this solution leads to linearized equations with a matrix $\mathcal{L}$, which admits an irreducible representation in the form

$$\mathcal{L}=\mathcal{L}_1\{\rho_{22},\rho_{yy},\rho_{00},\rho_{xx},\mathrm{Im}(\rho_{2x})\}\oplus\mathcal{L}_2\{\rho_{11}\}\oplus\mathcal{L}_3\{\mathrm{Im}(\rho_{2y}),\mathrm{Re}(\rho_{xy})\}\oplus\mathcal{L}_4\{\mathrm{Im}(\rho_{1x}),\mathrm{Re}(\rho_{21}),\alpha_x\}\oplus\mathcal{L}_5\{\mathrm{Im}(\rho_{1y}),\alpha_y\},$$

where the variables within curly brackets indicate the subspace in which each submatrix $\mathcal{L}_i$ ($i=1-5$) is defined. Only $\mathcal{L}_4$ and $\mathcal{L}_5$ admit eigenvalues with positive real parts. Since the variables α_x and α_y lie in different submatrices, it turns out that the natural low-intensity solutions of the system will correspond to laser fields linearly polarized in the x or y directions. For submatrix $\mathcal{L}_4$ a real eigenvalue changes from negative to positive when the pump amplitude β reaches a threshold value $\beta_{\mathrm{th}(\|)}$ given by

$$\beta^2_{\mathrm{th}(\|)}=\{(g-\kappa_x\gamma_\perp)[3\gamma_c\gamma_\|+2\gamma_\perp(2\gamma_c+\gamma_\|)]-2\kappa_x\gamma_\perp^2(2\gamma_c+\gamma_\|)\pm B^{1/2}\}/8\kappa_x(2\gamma_c+\gamma_\|), \quad (5)$$

where

$$B=g^2[2\gamma_c\gamma_\perp+\gamma_\|(4\gamma_\perp+3\gamma_c)]^2+\kappa_x^2\gamma_\perp^2[8\gamma_c\gamma_\perp+\gamma_\|(4\gamma_\perp-3\gamma_c)]^2-2g\kappa_x\gamma_\perp\{[4\gamma_c\gamma_\perp+\gamma_\|(4\gamma_\perp+3\gamma_c)]+2\gamma_c\gamma_\perp\gamma_\|(4\gamma_\perp+3\gamma_c)\}. \quad (6)$$

At $\beta=\beta_{\mathrm{th}(\|)}$ the zero-intensity solution loses its stability through a pitchfork bifurcation, $PB_\|$, which gives rise to a steady-state solution with linear polarization in the x direction. This solution will be denoted as a ''parallel'' solution, since its polarization is parallel to that of the pumping field. Similarly, the submatrix $\mathcal{L}_5$ yields a pitchfork bifurcation, $PB_\perp$, at a pump value $\beta_{\mathrm{th}(\perp)}$ given by

$$\beta^2_{\mathrm{th}(\perp)}=3\gamma_\perp^2\gamma_c\gamma_\|\kappa_y/[2g(\gamma_c-\gamma_\|)-4\kappa_y\gamma_\perp(2\gamma_c+\gamma_\|)], \quad (7)$$

which leads to the appearance of a steady-state solution linearly polarized in the y direction, to be denoted as ''orthogonal'' solution. The smallest of these two pump thresholds, $\beta_{\mathrm{th}(\|)}$ or $\beta_{\mathrm{th}(\perp)}$, defines the so-called ''first laser threshold.'' Notice that for $\beta_{\mathrm{th}(\|)}$ two solutions are found [term $\pm B^{1/2}$ in Eq. (5)]; here we will only consider the smallest of these two solutions (i.e., the one with the term $-B^{1/2}$). The other solution (term $+B^{1/2}$) corresponds to another pitchfork bifurcation, which describes the disappearance of the parallel solution at very large pumping as a result of the ac Stark shift induced by the strong pump field on the upper-level manifold [26] (more details to be given elsewhere; in this paper only the more accessible regime of small pump power will be considered).

For the sake of completeness, it must be pointed out that in the case of the submatrix $\mathcal{L}_4$ one or two Hopf bifurcations can also be found. These bifurcations are similar to the ones reported in [26], but in the case of our laser system they appear at very large pumping strengths and only for a limited domain of parameter values, so that they will be ignored here.

B. Steady-state solution

An exact analytical expression for the parallel and orthogonal steady-state solutions can be obtained from Eqs. (3) (use of symbolic mathematics software is convenient). For the sake of brevity we only give here the expression for the laser field amplitudes α_x (parallel solution) and α_y (orthogonal solution):

$$\alpha_x=\{[(C^2+D)^{1/2}-C]/8\kappa_x\gamma_\|(2\gamma_c+\gamma_\|)\}^{1/2}, \quad (8)$$

$$\alpha_y=(1/2)\{[\gamma_c\gamma_\|\{2\beta^2[g(\gamma_c-\gamma_\|)-2\kappa_y\gamma_\perp(2\gamma_c+\gamma_\|)]-3\gamma_c\gamma_\|\gamma_\perp^2\kappa_y\}]/\kappa_y\{\beta^2[\gamma_c(5\gamma_c+6\gamma_\|)+\gamma_\|^2]+\gamma_c\gamma_\|\gamma_\perp(2\gamma_c+\gamma_\|)\}\}^{1/2}, \quad (9)$$

where

$$C=\kappa_x\{4\beta^2[\gamma_\perp(5\gamma_c+4\gamma_\|)-\gamma_\|(\gamma_c+2\gamma_\|)]+\gamma_\|\gamma_\perp[\gamma_\|(3\gamma_c+4\gamma_\perp)+8\gamma_c\gamma_\perp]\}$$

$$D=16\gamma_\|^2\kappa_x(2\gamma_c+\gamma_\|)\{\beta^2\{g[3\gamma_c\gamma_\|+2\gamma_\perp(\gamma_c+2\gamma_\|)]-4\beta^2\kappa_x(2\gamma_c+\gamma_\|)-\kappa_x\gamma_\perp[3\gamma_c\gamma_\|+4\gamma_\perp(2\gamma_c+\gamma_\|)]\}-3\gamma_c\gamma_\|\gamma_\perp^3\kappa_x\}. \quad (10)$$

Figure 1 shows, in a particular case, the dependence of the emission intensity I ($I=\alpha_x^2+\alpha_y^2$) on the pump field amplitude β, for the parallel and orthogonal solutions. In the domain of small β here considered ($\beta\ll\gamma_\perp$) there is an approximately linear dependence of the emission intensity I on the pump power (β^2) for both the parallel and orthogonal solutions, which means that pump saturation effects are negligible.

Comparison of Eq. (5) with (7) [or Eq. (8) with (9)] shows that for cavity losses $\kappa_x\sim\kappa_y$ the pump threshold for the parallel solution is always much smaller than the threshold for the orthogonal solution, $\beta_{\mathrm{th}(\|)}<\beta_{\mathrm{th}(\perp)}$. This is in agreement with what was found in [13], in the sense that the laser system, in the absence of cavity-loss anisotropy, has preference for the parallel solution (through a pump-induced gain anisotropy). However, by increasing the ratio κ_x/κ_y (or by increasing γ_c) one can compensate for the gain anisotropy and obtain a lower threshold for the orthogonal solution, i.e., $\beta_{\mathrm{th}(\perp)}<\beta_{\mathrm{th}(\|)}$. This is what occurs in the examples of Fig. 2. The border point between the two situations is when $\beta_{\mathrm{th}(\perp)}=\beta_{\mathrm{th}(\|)}$, which according to Eqs. (5) and (7) requires

$$\kappa_x/\kappa_y=\{[\gamma_\|(3\gamma_c+4\gamma_\perp)+2\gamma_\perp\gamma_c][2\kappa_y\gamma_\perp(2\gamma_c+\gamma_\|)-g(\gamma_c-\gamma_\|)]\}/\{\gamma_\perp(\gamma_c-\gamma_\|)[4\kappa_y\gamma_\perp(2\gamma_c+\gamma_\|)-3\kappa_y\gamma_\|\gamma_c-2g(\gamma_c-\gamma_\|)]\}. \quad (11)$$

For class C lasers such as, for instance, far infrared lasers where $\gamma_\|/\gamma_\perp\sim\gamma_c/\gamma_\perp\sim1$ and $g/\gamma_\perp^2\sim10^3$ [27], the critical value of the ratio κ_x/κ_y becomes almost independent of κ_y:

$$\kappa_x/\kappa_y\simeq[\gamma_\|(3\gamma_c+4\gamma_\perp)+2\gamma_\perp\gamma_c]/[2\gamma_\perp(\gamma_c-\gamma_\|)], \quad (12)$$

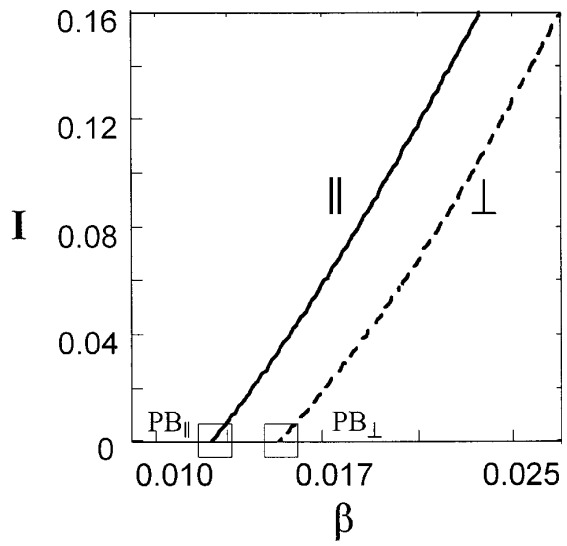

FIG. 1. Laser emission intensity for the parallel || ($I=\alpha_x^2$) and orthogonal ⊥ ($I=\alpha_y^2$) solutions, as a function of pump amplitude β. $PB_{\|}$ and $PB_{\perp}$ denote the corresponding pitchfork bifurcations. $\kappa_x=\kappa_y=0.4$, $\gamma_{\|}=0.28$, $\gamma_c=0.35$, g=3650 (decay rates and field amplitudes normalized to $\gamma_{\perp}$; g has been normalized to $\gamma_{\perp}^2$. Continuous (dashed) line denotes stable (unstable) solution.

whenever $\kappa_y/\gamma_{\perp}\lesssim 1$. Thus essentially the same result is obtained in cases of good or bad cavity conditions.

Condition (12) is represented in Fig. 3 on the plane κ_x/κ_y versus γ_c, for several values of $\gamma_{\|}$. Below a given one of these curves is $\beta_{th(\|)}<\beta_{th(\perp)}$, so that the parallel solution is generated at threshold, whereas above the curve the orthogonal solution is generated at threshold. With increasing the upper-level coherence relaxation rate γ_c the pump-induced gain anisotropy is reduced and a lower κ_x/κ_y ratio is required for generation of the orthogonal solution.

This behavior admits a simple interpretation in the ''linear'' basis of states $|x\rangle,|0\rangle,|y\rangle$. The pump field linearly polarized in the x direction only excites the $|x\rangle$ substate in the $J=1$ upper-level manifold. Thus, in principle, the maximum gain will correspond to a laser field linearly polarized in the x direction, since it directly connects the $|x\rangle$ substate with the lower-energy $J'=0$ state. Gain for the field linearly polarized in the y direction only exists in the measure that the internal relaxation mechanisms within the $J=1$ upper-level manifold, in particular the γ_c relaxation rate, transfers population from the $|x\rangle$ state to the $|y\rangle$ state. This is the reason why, according to Eq. (7), $\beta_{th(\perp)}^2\to\infty$ when γ_c decreases to a critical value $\widetilde{\gamma_c}$ given by

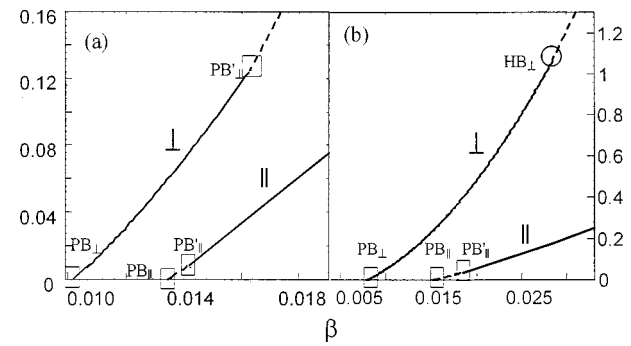

FIG. 2. The same as in Fig. 1, except for $\kappa_x=4$ and (a) $\gamma_c=0.5$, (b) $\gamma_c=1$. $HB_{\perp}$ denotes a Hopf bifurcation.

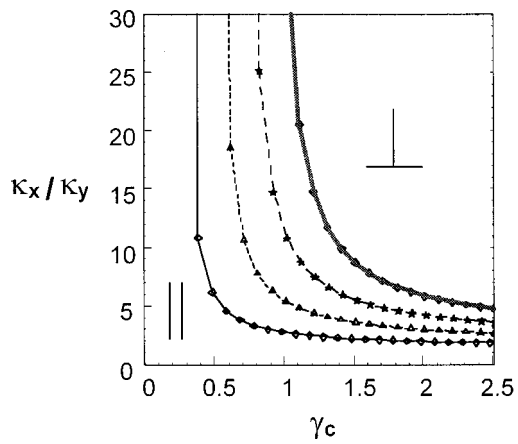

FIG. 3. Curves in parameter space defining the points where the pump thresholds for parallel and orthogonal solutions coincide. From left to right, the curves correspond to $\gamma_{\|}=0.28$, 0.5, 0.7, and 0.9, respectively (other parameters as in Fig. 1).

$$\widetilde{\gamma_c}=\gamma_{\|}[(g+2\kappa_y\gamma_{\perp})/(g-2\kappa_y\gamma_{\perp})] \tag{13}$$

(which becomes $\widetilde{\gamma_c}\simeq\gamma_{\|}$ for $g\gg\kappa_y\gamma_{\perp}$) [28]. In its turn, this explains the vertical asymptotic behavior of the curves in Fig. 3 for decreasing γ_c.

A linear stability analysis of the parallel and orthogonal solutions (performed with symbolic mathematics software) leads to a linearized matrix which in the case of the orthogonal solution can be factorized in the form $\mathcal{L}_1'\{\rho_{11},\rho_{22},\rho_{xx},\rho_{00},\rho_{yy},\mathrm{Im}(\rho_{2x}),\mathrm{Im}(\rho_{1y}),\alpha_y\}\oplus\mathcal{L}_2'\{\mathrm{Re}(\rho_{xy}),\mathrm{Im}(\rho_{1x}),\mathrm{Im}(\rho_{2y}),\mathrm{Re}(\rho_{21}),\alpha_x\}$. The final results of the analysis of both solutions are the following: (i) When $\beta_{th(\|)}<\beta_{th(\perp)}$ (i.e., below curve in Fig. 3) only the parallel solution is stable, for any value of β (within the domain $\beta<\gamma_{\perp}$ here considered). This is the case for the example of Fig. 1. (ii) When $\beta_{th(\perp)}<\beta_{th(\|)}$ (i.e., above curve in Fig. 3) the orthogonal solution is born stable but at a certain value of the pump-field amplitude β it loses its stability through a subcritical pitchfork bifurcation [$PB_{\perp}'$ point in Fig. 2(a)] which affects the submatrix $\mathcal{L}_2'$. On the other hand, the parallel solution, which is unstable near its threshold $\beta_{th(\|)}$, becomes stable through another subcritical pitchfork bifurcation, followed in inverse sense [$PB_{\|}'$ point in Fig. 2(a)]. The $PB_{\|}'$ bifurcation occurs at a value of β smaller than that corresponding to the $PB_{\perp}'$ bifurcation.

Thus in case (ii), by continuously increasing β, the system ''switches'' at the $PB_{\perp}'$ point from parallel to orthogonal solution. As can be seen in Fig. 2(a), there is hysteresis and a domain of bistability between the two solutions exists. This polarization switching phenomenon violates the so-called ''maximum emission principle'' (an empirical rule that is often found in multimode laser physics [29]) in the sense that for increasing β switching at $PB_{\perp}'$ occurs from one steady-

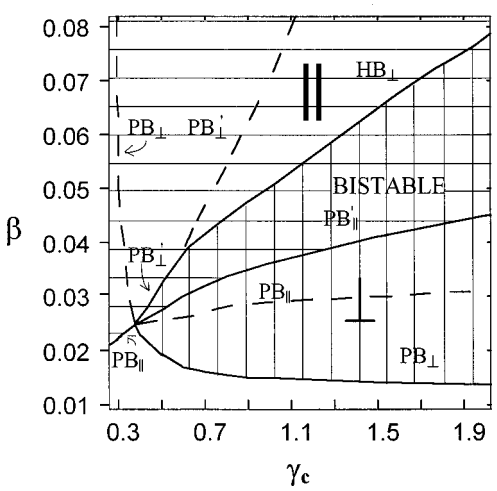

FIG. 4. Phase space diagram in the (γ_c,β) parameter plane ($J=1$ manifold coherence vs pump amplitude), showing the domains of stable parallel $||$ (horizontal line area) and orthogonal $\perp$ (vertical line area) emission. $\kappa_x=14.25$, $\kappa_y=1.425$, $\gamma_\parallel=0.28$, $g=3650$. The smallest possible value for γ_c is $\gamma_c=\gamma_\parallel=0.28$.

state solution to another of much smaller intensity, Fig. 2(a). The origin of this behavior is difficult to establish with precision, but in principle it is related with the fact that parallel emission involves pumping through two-photon (Raman) processes, which are absent in the case of orthogonal emission.

The orthogonal solution is also affected by a subcritical Hopf bifurcation associated with the matrix $\mathcal{L}_2'$, but it only exists for values of γ_c above a certain threshold. (iii) With increasing γ_c (keeping κ_x and κ_y fixed), the position of the $PB_\perp'$ point on the orthogonal polarization branch [Fig. 2(a)] moves rapidly toward higher values of pumping strength β, thus increasing the width of the bistability domain. For large enough γ_c, the Hopf bifurcation appears at a pump threshold smaller than that of $PB_\perp'$, so that switching from the orthogonal solution to the parallel solution occurs now at this Hopf bifurcation point [$HB_\perp$ point in Fig. 2(b)] instead of at the $PB_\perp'$ point.

Figure 4 shows a complete phase diagram on the $(\gamma_c,\ \beta)$ plane, for a fixed value of the cavity loss ratio, $\kappa_x/\kappa_y=10$. All the features discussed in Figs. 1 and 2 also show up in Fig. 4. For $\gamma_c<0.38$, the pump threshold for the parallel solution ($PB_\parallel$ line) is lower than for the orthogonal solution ($PB_\perp$ line). The $PB_\perp$ threshold tends to infinity when γ_c decreases down to the critical value $\tilde{\gamma}_c\simeq\gamma_\parallel$ given by Eq. (13). For $\gamma_c>0.38$, the lowest pump threshold corresponds to the orthogonal solution. The position of the $PB_\perp'$, $PB_\parallel'$, and $HB_\perp$ points is also shown by the corresponding curves. A stable parallel (orthogonal) solution exists in the area lined horizontally (vertically). Overlapping between these two areas defines the domain of bistability. In this domain perturbations can make the system switch from one solution to the other; the parallel solution is more robust against perturbations than the orthogonal solution; the robustness of this last solution increases with increasing γ_c.

It is worth noting that the $HB_\perp$ branch does not cross the $PB_\perp'$ branch; with decreasing γ_c, the $HB_\perp$ branch approaches tangentially the $PB_\perp'$ branch and dissapears. Related to this, it is also observed that the two complex-conjugate eigenvalues with positive real part that arise at the $HB_\perp$ branch exist only in the domain in Fig. 4 delimited by the branches $HB_\perp$ and $PB_\perp'$; above the $PB_\perp'$ branch, there is only one (real) eigenvalue with positive real part (the one associated with the $PB_\perp'$ bifurcation).

IV. CONCLUSIONS

In conclusion, we have shown in this paper that the polarization behavior of a resonant $J=1\rightarrow J'=0$ laser in the case of coherent pumping with a linearly polarized field is very different from that reported in the case of incoherent pumping. The strong nonlinear gain anisotropy induced by the polarized pump field is influenced by the values of the relaxation rates $\gamma_\parallel$ and γ_c, but it is not influenced at all by the value of γ_J. Thus, the sensitivity of polarization effects to this parameter found for an incoherently pumped laser [6,7] has no counterpart here. This sensitivity could only be found, to some degree, in cases of pumping with fields in other polarization states. Excluding external modulation of laser parameters, the most efficient way to affect the polarization state of the laser field is by introducing large cavity-loss anisotropies, which can compensate the strong gain for the parallel solution making possible generation of the orthogonal solution. This, however, can only be achieved at small pump-field amplitudes; with increasing pumping the system switches to the parallel solution, in spite of the fact that this switching results in a strong decrease in the emission intensity that violates the so-called maximum emission principle. A domain of bistability between the parallel and orthogonal solutions is found, whose width increases with increasing the decay rate of the coherence induced by the pump field in the upper level $J=1$ manifold.

No other stable solutions, with polarization different from (linear) parallel or orthogonal, have been found. The bifurcation points $PB_\perp'$ and $PB_\parallel'$ in Fig. 2(a) are connected by an unstable branch of solutions with linear polarization at angles different from 0 or $\pi/2$ with respect to the x axis. Differently from the case of the incoherently pumped $J=1\rightarrow J'=0$ laser [6,7], no stationary solution, neither stable or unstable, with ellipticity different from zero exists.

All these polarization features appear at small values of the pump strength, which are obviously the most easily achievable and convenient operating conditions in practice. Nevertheless, it would also be interesting to investigate the polarization dynamics at larger pump strengths, where time-dependent solutions appear and preference for parallel polarization might be less strong, or at non-null cavity detunings. Possibly complex polarization states could be found in both cases.

ACKNOWLEDGMENTS

We acknowledge with thanks Neal B. Abraham for his suggestions and critical reading of the manuscript. C.S. gratefully acknowledges Josep L. Font for his assistance in computer matters. Financial support from the Spanish DGICYT under Contract No. PB95-0778-C02-01 is acknowledged.

[1] H. de Lang and G. Bouwhuis, Phys. Lett. **19**, 481 (1965); D. Polder and W. Van Haeringen, Phys. Lett. **19**, 380 (1965).
[2] R. L. Fork and M. Sargent III, Phys. Rev. **139**, A617 (1965); M. Sargent III, W. E. Lamb, Jr., and R. L. Fork, Phys. Rev. **164**, 436 (1967).
[3] G. Stéphan, A. D. May, R. E. Mueller, and B. Aissaoui, J. Opt. Soc. Am. B **4**, 1276 (1987).
[4] A. P. Voitovich, L. P. Svirina, and V. N. Severikov, Opt. Commun. **80**, 435 (1991); L. P. Svirina, *ibid.* **111**, 370 (1994).
[5] X. W. Xia, W. J. Sandle, R. J. Ballagh, and D. M. Warrington (unpublished).
[6] N. B. Abraham, E. Arimondo, and M. San Miguel, Opt. Commun. **117**, 344 (1995); **117**, 244 (1995).
[7] M. D. Matlin, R. S. Gioggia, N. B. Abraham, P. Glorieux, and T. Crawford, Opt. Commun. **120**, 204 (1995); N. B. Abraham, M. D. Matlin, and R. S. Gioggia, Phys. Rev. A **53**, 3514 (1996).
[8] J. Redondo, E. Roldán, and G. J. de Valcárcel, Phys. Lett. A **210**, 301 (1996).
[9] G. P. Puccioni, M. V. Tratnik, J. E. Sipe, and G. L. Oppo, Opt. Lett. **12**, 242 (1987).
[10] R. J. Ballagh and N. J. Mulgan, Phys. Rev. A **52**, 4945 (1995).
[11] J. C. Cotteverte, F. Bretenaker, A. Le Floch, and P. Glorieux, Phys. Rev. A **49**, 2868 (1994).
[12] M. Arjona, R. Corbalán, F. Laguarta, J. Pujol, and R. Vilaseca, Phys. Rev. A **41**, 6559 (1990); R. Corbalán, R. Vilaseca, M. Arjona, J. Pujol, E. Roldán, and G. J. de Valcárcel, Phys. Rev. A **48**, 1483 (1993).
[13] C. Serrat, A. Kul'minskii, R. Vilaseca, and R. Corbalán, Opt. Lett. **20**, 1353 (1995).
[14] S. Bielawski, D. Derozier, and P. Glorieux, Phys. Rev. A **46**, 2811 (1992).
[15] B. Meziane, F. Sánchez, and G. M. Stéphan, Opt. Lett. **19**, 1970 (1994).
[16] Q. L. Williams, J. García-Ojalvo, and R. Roy, Phys. Rev. A **55**, 2376 (1997).
[17] M. San Miguel, Q. Feng, and J. V. Moloney, Phys. Rev. A **52**, 1728 (1995).
[18] C. Serrat, N. B. Abraham, M. San Miguel, R. Vilaseca, and J. Martín-Regalado, Phys. Rev. A **53**, R3731 (1996).
[19] M. Travagnin, M. P. van Exter, A. K. Jansen van Doorn, and J. P. Woerdman, Phys. Rev. A **54**, 1647 (1996).
[20] F. Robert, P. Besnard, M. L. Charés, and G. M. Stéphan, Opt. Quantum Electron. **27**, 805 (1995).
[21] Y. Ozeki and C. L. Tang, Appl. Phys. Lett. **58**, 2214 (1991).
[22] L. Gil, Phys. Rev. Lett. **70**, 162 (1991).
[23] M. San Miguel, Phys. Rev. Lett. **75**, 425 (1995).
[24] A. Kul'minskii, R. Vilaseca, and R. Corbalán, Opt. Lett. **20**, 2390 (1995).
[25] D. Lenstra, Phys. Rep. **59**, 299 (1980).
[26] J. V. Moloney, J. S. Uppal, and R. G. Harrison, Phys. Rev. Lett. **59**, 2868 (1987).
[27] C. O. Weiss and R. Vilaseca, *Dynamics of Lasers* (VCH, Weinheim, 1991).
[28] A similar result was found, with a slightly different model, in E. Roldán, J. G. de Valcárcel, R. Vilaseca, and R. Corbalán, Phys. Rev. A **49**, 1487 (1994).
[29] C. L. Tang and H. Statz, J. Appl. Phys. **38**, 2963 (1967).